Glavonoid-rich oil supplementation reduces stearoyl-coenzyme A desaturase 1 expression and improves systemic metabolism in diabetic, obese KK-A^y mice

Yuichi Igarashi [a], Shiho Iida [a], Jian Dai [b], Jia Huo [a,c], Xiaoran Cui [a], Jinko Sawashita [d], Masayuki Mori [b,e], Hiroki Miyahara [b], Keiichi Higuchi [b,e,f,*]

[a] Department of Aging Biology, Shinshu University Graduate School of Medicine, Matsumoto, Japan
[b] Department of Neuro-Health Innovation, Institute for Biomedical Sciences, Interdisciplinary Cluster for Cutting Edge Research, Shinshu University, Matsumoto, Japan
[c] The Third Hospital of Hebei Medical University, Shijiazhuang, China
[d] Research & Development Team, Supplement Business Division, Pharma & Supplemental Nutrition Solutions Vehicle, Kaneka Corporation, Osaka, Japan
[e] Department of Aging Biology, Shinshu University School of Medicine, Matsumoto, Japan
[f] Community Health Care Research Center, Nagano University of Health and Medicine, Nagano, Japan

ARTICLE INFO

ABSTRACT

Aims: Glavonoid-rich oil (GRO) derived from ethanol extraction of licorice (*Glycyrrhiza glabra Linne*) root has been reported to have beneficial effects on health. In this study, we aimed to determine the effect of long-term administration of GRO on metabolic disorders and to elucidate the molecular mechanism.

Main methods: Female obese, type 2 diabetic KK-A^y mice were fed diets supplemented with 0.3% or 0.8% GRO (w/w) for 4–12 weeks. Mice were euthanized and autopsied at 20 weeks old. The effects of GRO on lipid and glucose metabolism were evaluated by measuring physiological and biochemical markers using mRNA sequencing, quantitative reverse-transcription PCR, and western blot analyses.

Key findings: Compared to mice fed the control diet, GRO-supplemented mice had reduced body and white adipose tissue weights, serum levels of triglycerides and cholesterol, and improved glucose tolerance, while food intake was not affected. We found remarkable reductions in the gene expression levels of stearoyl-coenzyme A desaturase 1 (*Scd1*) and pyruvate dehydrogenase kinase isoenzyme 4 (*Pdk4*) in the liver, in addition to decreased expression of fatty acid synthase (*Fasn*) in inguinal white adipose tissue (iWAT). These results suggest that GRO supplementation improves lipid profiles via reduced de novo lipogenesis in the liver and white adipose tissue. Glucose metabolism may also be improved by increased glycolysis in the liver.

Significance: Our analysis of long-term supplementation of GRO in obese and diabetic mice should provide novel insight into preventing insulin resistance and metabolic syndromes.

1. Introduction

Metabolic disorders caused by obesity and overeating have become a global health problem [1]. Obesity is a critical risk factor for various metabolic disorders, including insulin resistance and type 2 diabetes. Diabetes is estimated to affect 300 million people worldwide by 2025 [2]. Increasing evidence suggests that a longer life span and changes in dietary habits and lifestyle are external risk factors, and that hyperglycemia, hyperlipidemia, obesity, high blood pressure, mitochondrial dysfunction, chronic inflammation, and oxidative stress are internal risk

factors [3–7]. Frailty has been associated with degeneration of skeletal muscle mass and strength associated with aging [8] and is considered a high-risk factor for adverse health outcomes. Thus, development of medicine or supplement for metabolic disorders is required.

Licorice (*Glycyrrhiza glabra Linne*) is a medicinal herb commonly used worldwide, and its root extract and major functional compound, glabridin, have been reported to exert beneficial effects on obesity, oxidative stress, and tumors [9–14]. Many studies have revealed the lack of toxicity of licorice and its effects on decreasing body and adipose tissue weights, blood glucose levels, and oxidative stress and increasing

lipid and glucose metabolism and muscle mass in experimental animals and humans [15–18]. Glavonoid-rich oil (GRO) is derived from ethanol extraction of licorice root and dissolved in medium chain triglyceride oil (MCT). GRO contains various hydrophobic flavonoids, among which glabridin is the major active constituent. The molecular mechanism of these health-promoting effects of GRO may depend on activation of peroxisome proliferator-activated receptor (PPAR) γ, mammalian target of rapamycin, and adenosine monophosphate activated protein kinase (AMPK) pathways [19–21]. However, the mechanism by which GRO mitigates obesity and insulin resistance has not been elucidated completely.

KK mice were established from wild-derived ddY mice as a mildly obese, insulin-resistant mouse model. The KK-A^y congenic mouse is developed by transferring the yellow obese syndrome-associated agouti gene (A^y allele) into KK mouse [22]. Ectopic expression of the agouti protein antagonizes melanocortin receptor 4 in the hypothalamus and induces overeating, obesity, and insulin resistance. KK-A^y mice have more severe obesity and hyperglycemia compared with KK mice. Thus, KK-A^y mice are widely used as a valuable model for investigating treatments for type 2 diabetes, obesity, and disorders associated with impaired lipid and glucose metabolism [23–25].

Here, we investigated the health-promoting effects of relatively long-term, high-dose GRO supplementation on obesity and insulin resistance using KK-A^y mice. Also, we performed mRNA sequencing (RNA-Seq) analysis to identify a novel molecular mechanism underlying the effects of GRO treatment on improvements of weight gain and glucose/lipid metabolism.

2. Materials and methods

2.1. Animals

Seven-week-old female KK-A^y mice were purchased from CLEA Japan, Inc. (Tokyo, Japan). The animals were raised in the Division of Animal Research, Research Center for Supports to Advanced Science, Shinshu University under specific pathogen-free conditions at 24 ± 3 °C and a controlled light regimen (12 h light/dark cycle). Tap water was provided ad libitum.

After a 1-week acclimation period on a commercial diet, CE-2 (CLEA, Japan), 8-week-old KK-A^y mice were weighed and randomly assigned to three groups to avoid significant differences in body weight among the groups and housed five per cage without regrouping. Mice (n = 20) in the control group (Cont) were fed CE-2 mixed with 0.8% (w/w) MCT oil (Fujifilm Wako Chemicals, Osaka, Japan), and mice in the 0.3% GRO (n = 20) and 0.8% GRO (n = 20) groups were fed CE-2 supplemented with 0.3% GRO (w/w) and 0.8% GRO (w/w), respectively, starting at 8 weeks of age. All mice were given free access to food and water. Mice were inspected daily, and body weight was recorded once a week. Food was changed twice a week, and food intake was calculated once a week.

Intraperitoneal glucose tolerance test was performed 12, 16, or 20 weeks of age after fasted for 12 h (21:00–9:00) and then given an intraperitoneal injection of glucose (1 g/kg body weight) 2 days before euthanasia and autopsy. Blood samples were collected at 0, 15, 30, 60, 90, 120, or 180 min after glucose injection for blood glucose measurements. Blood glucose levels were measured using the Accu-Chek Aviva glucose monitor (Roche, Indianapolis, IN, USA). Before sacrifice at 8, 12, 16, or 20 weeks of age, mice in each group were fasted for 12 h, and were deeply anesthetized with sevoflurane (Fujifilm Wako Chemicals) followed by cardiac puncture and collection of blood and organs. Serum was isolated after coagulation by centrifugation at 3000 g for 10 min at room temperature. The major organs, inguinal white adipose tissue (iWAT), and several muscles of the hind limbs (quadriceps, tibialis anterior, extensor digitorum longus, gastrocnemius, soleus, and plantaris) were collected and weighed. Half of the collected organs and the muscles of the left limbs were frozen at -80 °C, and the other half of the organs and the muscles of the right limbs were fixed in 10% neutral buffered formalin.

Serum insulin levels were measured by ELISA (LBIS Mouse Insulin ELISA Kit, Fujifilm Wako Chemicals) according to the manufacturer's instructions. Serum triglyceride and total and HDL cholesterol levels were measured using enzymatic kits (Fujifilm Wako Chemicals).

The protocols for the animal experiments were reviewed by the Committee for Animal Experiments and finally approved by the president of Shinshu University (Approval Number 280016).

2.2. GRO-containing feed

Licorice root was extracted using 95% ethanol, followed by filtration and concentration. The ethanol extracts were mixed with MCT oil (fatty acid composition: 99:1 C8:C10), and the concentration of glabridin, a major constituent, was adjusted to 3%. This extract was used in this study as GRO. GRO consists of various lipid soluble flavonoids, including glabridin as the major active component. GRO contains less than 0.0005% hydrophilic glycyrrhizic acid, which may induce high blood pressure or hypocalcemia (Kaneka, Osaka, Japan). The control pellet feed was prepared by mixing the CE-2 commercial diet with 0.8% MCT (w/w), and the experimental feeds were prepared by mixing CE-2 with 0.3% or 0.8% GRO (w/w).

2.3. Pathological analysis

The formalin-fixed organs were embedded in paraffin and cut into 4-μm-thick sections using standard procedures. The sections were stained with hematoxylin and eosin (HE). Five areas within each HE-stained section of iWAT from five 20-week-old mice were randomly photographed at 200× magnification, and the adipocyte size was determined using the ImageJ software (NIH, Bethesda, MD, USA). To count cells in the stromal vascular fraction, five randomly selected regions in five iWAT sections stained with 4′,6-diamidino-2-phenylindole (DAPI) were photographed at 200× magnification. The number of stained nuclei was calculated using the ImageJ software.

2.4. RNA-Seq analysis

Cont and 0.8% GRO mice of 12 and 20 weeks of age (4 groups, n = 5 each) were subjected to the RNA-Seq analysis. Frozen liver samples were thawed, and pieces (~ 10 mg) of the sample of the groups were pooled into a single tube. The pooled liver samples were homogenized in TRIzol RNA isolation reagent (Invitrogen/Thermo Fisher Scientific, Tokyo, Japan). The homogenized samples were sent to Filgen (Nagoya, Japan) for RNA-Seq using an Illumina next-generation sequencing platform after confirming the RNA quality using the Bioanalyzer 2100 (Agilent Technology, Santa Clara, CA, USA). The count data from sequencing were analyzed using DESeq2 software to determine the genes that were significantly differentially expressed among the groups. Biological functions associated with the differentially expressed genes were analyzed using the gene ontology and KEGG pathway annotation databases, to elucidate the effects of GRO supplementation.

2.5. qRT-PCR

Total RNA was extracted from the liver, iWAT, and quadriceps muscles using TRIzol reagent followed by a treatment with the DNA-Free DNA Removal Kit (Invitrogen/Thermo Fisher Scientific). The RNA was then subjected to reverse transcription using the High Capacity cDNA Reverse Transcription Kit with random primers (Invitrogen/Thermo Fisher Scientific). qRT-PCR was performed using SYBR Green Premix EX Taq™ II (Takara Bio, Tokyo, Japan), and the reactions were run on the ABI Prism 7500 Sequence Detection System (Applied Biosystems/Thermo Fisher Scientific, Tokyo, Japan). A housekeeping β-actin gene was primarily used for normalization of gene expression. For genes that showed significant changes in expression following

Table 1
Primer pairs used for qRT-PCR.

Gene	Forward (5′-3′)	Reverse (5′-3′)
Acacb	GGTAGTGGCTTTGAAGGAACTGTC	GATATCGTTGTTCTGGAAGCTCTCG
Acadm	AACACTTACTATGCCTCGATTGCA	CCATAGCCTCCGAAAATCTGCA
Acadvl	TCTGCAAGGCTGTATGGACA	CTGGGTGGACAATCCCTGAC
Acox1	CTGGTGGGTGGTATGGTGTC	TCTACCAATCTGGCTGCACG
Actb	ACAATGAGCTGCGTGTGGCC	CCTCGTAGATGGGCACAGTG
Adgre1	GATGAATTCCCGTGTTGTTGGT	ACATCAGTGTTCCAGGAGACACA
B2m	TGGTGCTTGTCTCACTGACC	AATGTGAGGCGGGTGGAACTG
Cd36	CAGCAATGAGCCCACAGTTCC	GTGCTGATCCTTTCAGAGTCTC
Ehhadh	TGGTGATTGGCACCCACTT	AGTATCGGCTAGGAATGACCTCTAGT
Elovl6	CGTCTTCAGTATATTCGGTGC	CCAGAATTTGCTGACAGGTC
Fasn	AGAGACGTGTCACTCCTGGACTT	GCTGCGGAAACTTCAGGAAAT
G6pc	ATGGTCACTTCTACTCTTGC	CAAGATGACGTTCAAACAC
Gck	GAATCTTCTGTTCCACGGAG	AGTGCTCAGGATGTTAAGGA
Il6	CCTCTCTGCAAGAGACTTCC	AGCCTCCGACTTGTGAAGTG
Irs1	ACGAACACTTTGCCATTGCC	CCTTTGCCCGATTATGCAGC
Lxr	CTCCTGATTCTGCAACGGAG	CCTAAAGCAACCCCAGTTGAC
Mlxipl	CTGGGGACCTAAACAGGAGC	GAAGCCACCCTATAGCTCCC
Pck1	GCATAACGGTCTGGACTTCT	TGATGACTGTCTTGCTTTCG
Pdk4	CACATGCTCTTCGGAACTCTTCAAG	TGATTGTAAGGTCTTCTTTTCCCAAG
Ppargc1a	TCACCACCGAAATCCTTA	GGTGTCTGTAGTGGCTTGAT
Ppara	GCGTACGGCAATGGCTTTAT	GAACGGCTTCTTCAGGTTCTT
Scd1	GAGGCCTGTACGGGATCATA	GCCGTGCCTTGTAAGTTCTGTG
Slc2a4	GGCTTTGTGGCCTTCTTTGAG	GACCCATAGCATCCGCAACAT
Srebf1	GGAGCCATGGATTGCACATT	GGCCCGGGAAGTCACTGT
Tnf	GTCCCCAAAGGGATGAGAAG	CCACTTGGTGGTTTGCTACG
18S	GTAACCCGTTGAACCCATTC	CCATCCAATCGGTAGTAGCG

normalization relative to β-actin, we verified the difference by normalization to two additional housekeeping genes (18S rRNA and β2-microglobulin) according to Minimum Information for Publication of Quantitative Real-Time PCR Experiments (MIQE) guidelines [26]. The primer sequences are listed in Table 1.

2.6. Western blot analysis

We measured protein levels by Western blot analysis as described previously [24]. Proteins from liver lysates (13 μg for evaluation of PPARα and β-actin, 50 μg for total and phosphorylated AMPKα1, and 100 μg for stearoyl-coenzyme A desaturase 1 (SCD1)) from each mouse were separated by SDS-PAGE using Tris-Tricine-SDS buffer and 12% polyacrylamide gels. After electrophoresis, the separated proteins were transferred to a polyvinylidene difluoride membrane (Immobilon, 0.2 μm pore, (Merck Millipore Burlington, MA, USA)) and incubated overnight at 4 °C with the following primary antibodies: polyclonal rabbit anti-mouse PPARα (1:3000, GeneTex, Los Angeles, CA, USA), β-actin (1:3000, GeneTex), total AMPKα1 (1:3000, GeneTex), phosphorylated AMPKα1 (Thr172) (1:1000, Cell Signaling Technology, Danvers, MA, USA), and SCD1 (1:1000, R&D Systems Minneapolis, MN, USA). The membranes were then incubated with horseradish peroxidase-conjugated anti-rabbit IgG (1:3000, Cell Signaling Technology) for 1 h at room temperature, and the target proteins were detected by enhanced chemiluminescence. Densitometric analysis of the target proteins was performed using the NIH ImageJ software.

2.7. Statistical analysis

All data are presented as means ± SD. Data were analyzed by Student's t-test, two-way ANOVA (Supplemental Table 1) or one-way ANOVA followed by Tukey's test, using R version 3.6.2 (The R Foundation for Statistical Computing). A p-value < 0.05 was considered to be statistically significant.

3. Results

3.1. GRO supplementation exhibit health-promoting effects in KK-A^y mice

We supplemented the diet with GRO to investigate the health-promoting effects of GRO in obese and diabetic KK-A^y mice. Body weight increased from ∼ 35 g at the start of treatment (8 weeks of age) to ∼ 59 g at the termination (20 weeks of age) in the Cont and 0.3% GRO groups (Supplemental Table 1). Body weight increased also in the 0.8% GRO group. However, it was significantly lower from age 11–20 weeks (Fig. 1A). Food intake (∼ 6 g/day) was constant during the 12 weeks of experimental period, and there was no statistical difference between groups at each age (Fig. 1B, Supplemental Table 1). This food intake was considerably higher compared to normal mice, suggesting that GRO did not influence the appetite or feeding activity of mice.

As for the organ weight, the iWAT was significantly lower in the 0.8% GRO group compared with the Cont group at all three ages (Fig. 2A, B). Also, the liver weight was significantly lower in the 0.8% GRO group compared with the Cont group, but the liver weight relative to body weight was not affected by GRO treatment (Fig. 2C, D). The weights of brown adipose tissue and other major organs were not affected by GRO supplementation (Fig. 2E–H and data not shown). Because enhanced muscle mass and muscle cell function by licorice extracts and glabridin have been reported [20,21], we measured the weights of several muscles in the hind limbs. The quadriceps weight relative to body weight was significantly higher in the 0.8% GRO group compared with the Cont group at age 16 and 20 weeks, but the quadriceps weight itself was not significantly different among the groups (Fig. 3A, B). We did not observe an effect of GRO on the weights of the soleus or other muscles (Fig. 3C, D and data not shown).

We observed tissue sections stained with HE for all mice and found no pathological abnormalities, including cancer and inflammation, in any of the mice in the three groups.

3.2. GRO supplementation improves a lipid profile of KK-A^y mice

To determine the effects of GRO on the adipocytes of iWAT from KK-A^y mice, iWAT specimens from 20-week-old mice in the Cont and 0.8% GRO groups were stained with HE. KK-A^y mice exhibited adipocyte
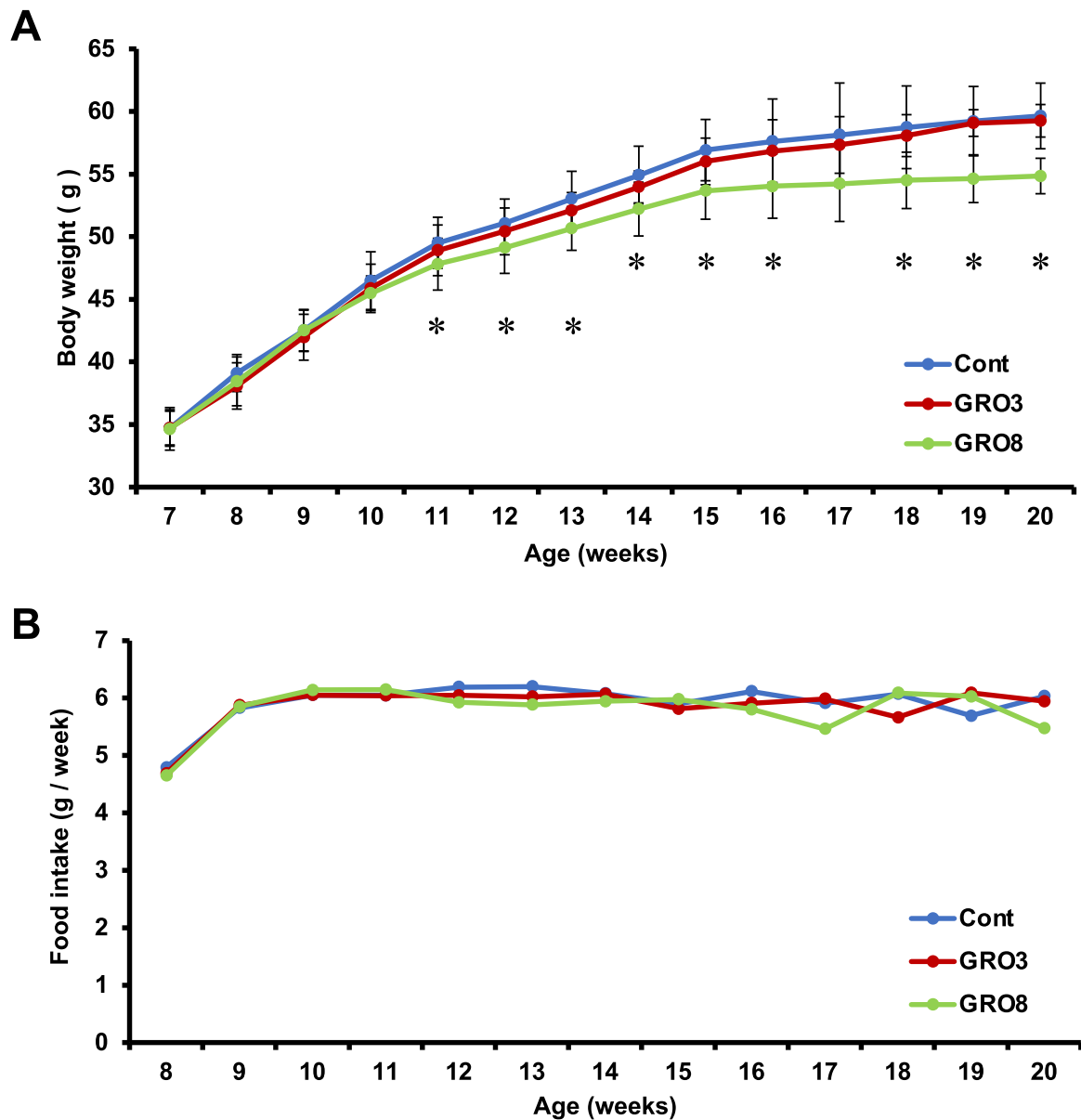
Fig. 1. GRO supplementation prevented the increase in body weight of KK-A^y mice without affecting food intake. (A) Body weight, (B) food intake (g/week). Cont: control mice; GRO3: 0.3% GRO mice; GRO8: 0.8% GRO mice. The data were analyzed with two-way ANOVA for independent variables, and subsequent one-way ANOVA followed by Tukey's test was performed for multiple comparisons. *$p < 0.05$, ** $p < 0.01$ compared with Cont mice. Values are means $\pm$ SD (n = 5–20).

hypertrophy, which was decreased by supplementation with 0.8% GRO (Fig. 4A), with a significantly increased proportion of smaller adipose cells (4001–8000 μm^2) and decreased proportion of larger cells (> 14,001 μm^2) compared with Cont mice (Fig. 4B). We observed a smaller number of stromal vascular fraction cells, including adipose tissue macrophages, in iWAT in 0.8% GRO mice compared with Cont mice (Fig. 4C). We also observed less fat accumulation in HE-stained liver sections in the 0.8% GRO group compared with the Cont group (Fig. 4D).

The development of obesity is often associated with abnormal lipid and glucose metabolism. We next addressed whether GRO supplementation improves metabolic function. Serum levels of total cholesterol and triglycerides were significantly lower in the 0.8% GRO than Cont groups at all three ages (Fig. 5A, C). Meanwhile, GRO supplementation did not affect the serum level of HDL cholesterol (Fig. 5B).

3.3. GRO supplementation improves glucose metabolism of KK-A^y mice

Next, we addressed whether GRO supplementation improves glucose metabolism. Mice supplemented with 0.8% GRO showed better glucose tolerance in an intraperitoneal glucose tolerance test at age 20 weeks (Fig. 6C). Glucose tolerance (represented by the area under the curve for blood glucose levels) did not change with age but was significantly greater in 0.8% GRO mice compared with Cont mice (Fig. 6D). The fasting serum glucose level suggested hyperglycemia (> 150 mg/dl), and 0.8% GRO supplementation tended to reduce this level, albeit not significantly (Fig. 6E). The fasting serum insulin level was decreased at age 16 weeks and increased at age 20 weeks, compared with age 12 weeks, but GRO supplementation did not affect this level (Fig. 6F). Together, these results indicate that 0.8% GRO migrates obesity and improves insulin resistance in KK-A^y mice.
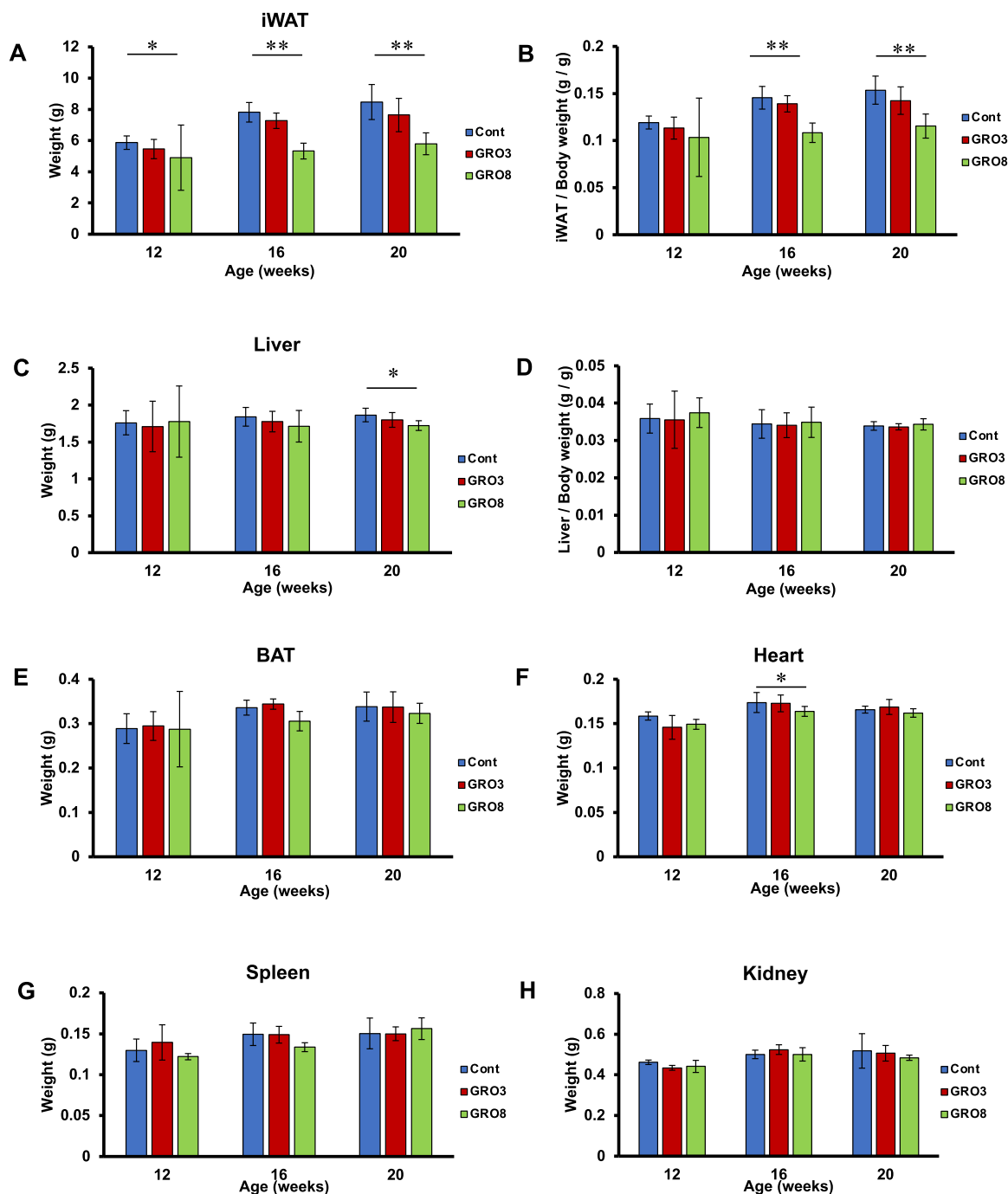
Fig. 2. GRO supplementation prevented the accumulation of visceral fat (iWAT) in KK-A^y mice. The weights of the (A) iWAT, (B) iWAT relative to body weight, (C) liver, (D) liver relative to body weight, (E) brown adipose tissue (BAT), (F) heart, (G) spleen, and (H) kidney. Cont: control mice; GRO3: 0.3% GRO mice; GRO8: 0.8% GRO mice. The data were analyzed with two-way ANOVA for independent variables, and subsequent one-way ANOVA followed by Tukey's test was performed for multiple comparisons. *$p < 0.05$, **$p < 0.01$. Values are means ± SD (n = 5).

3.4. GRO supplementation reduces expression of SCD1 and related genes in the liver of KK-A^y mice

To get insights into the molecular mechanisms of improvement in the lipid profile and glucose metabolism by GRO supplementation, we performed a transcriptome analysis of the liver, which plays a central role in lipid synthesis, by RNA-Seq. This analysis identified 54 significantly upregulated and 11 downregulated genes (Fig. 7). The biological functions of the differentially expressed genes were classified using annotation databases to elucidate the mechanism of the effects of GRO supplementation. Gene ontology analysis revealed that the differentially

expressed genes were significantly enriched in several pathways related to lipid metabolism (Table 2). Intriguingly, *Scd1* and *Ppara* were differentially expressed genes involved in all of these pathways.

We selected several genes involved in lipid and glucose metabolism (Table 3) and confirmed their differential expression in the liver between the 0.8% GRO and Cont mice at age 20 weeks using qRT-PCR. Of these genes, *Scd1* encodes an enzyme catalyzing the rate-limiting step in the synthesis of monounsaturated fatty acids (MUFAs) and triglycerides, specifically oleic acid from stearic acid, and is a key enzyme in fatty acid metabolism. SCD1 deficiency in the liver reduces triglyceride synthesis and blood triglyceride levels and mitigates obesity [27]. qRT-PCR
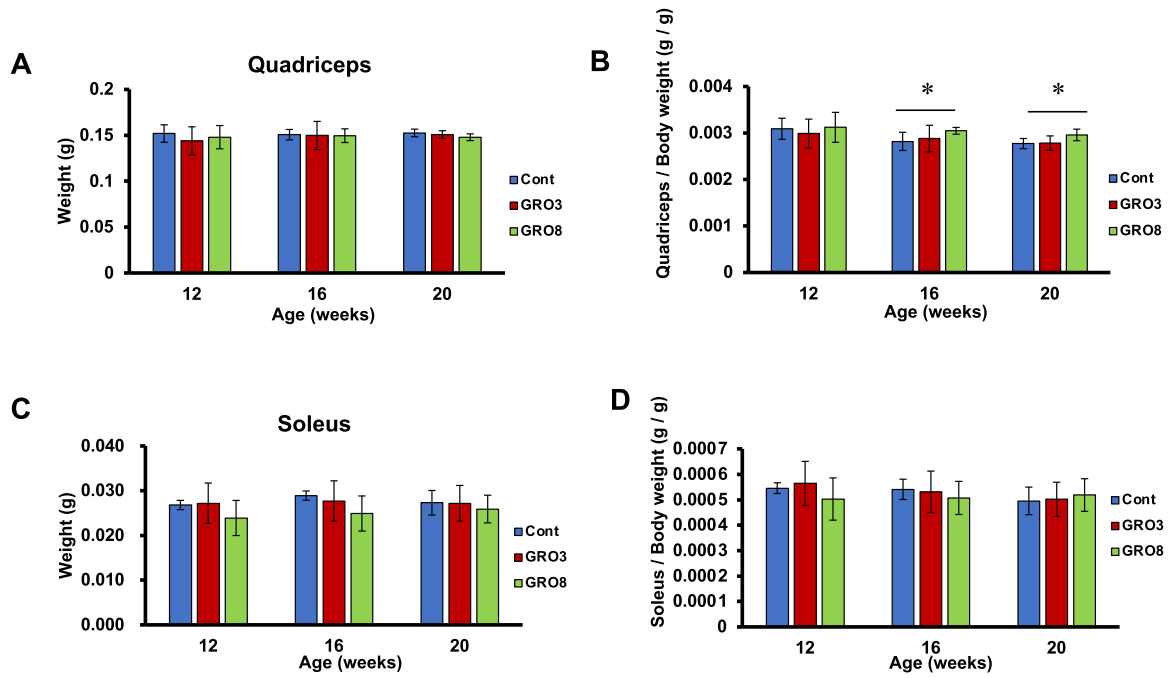
Fig. 3. GRO supplementation increased quadriceps muscle weights in KK-A^y mice. The weights of the (A) quadriceps, (B) quadriceps relative to body weight, (C) soleus, and (D) soleus relative to body weight. Cont: control mice; GRO3: 0.3% GRO mice; GRO8: 0.8% GRO mice. The data were analyzed with two-way ANOVA for independent variables, and subsequent one-way ANOVA followed by Tukey's test was performed for multiple comparisons. *$p < 0.05$. Values are means $\pm$ SD (n = 5).
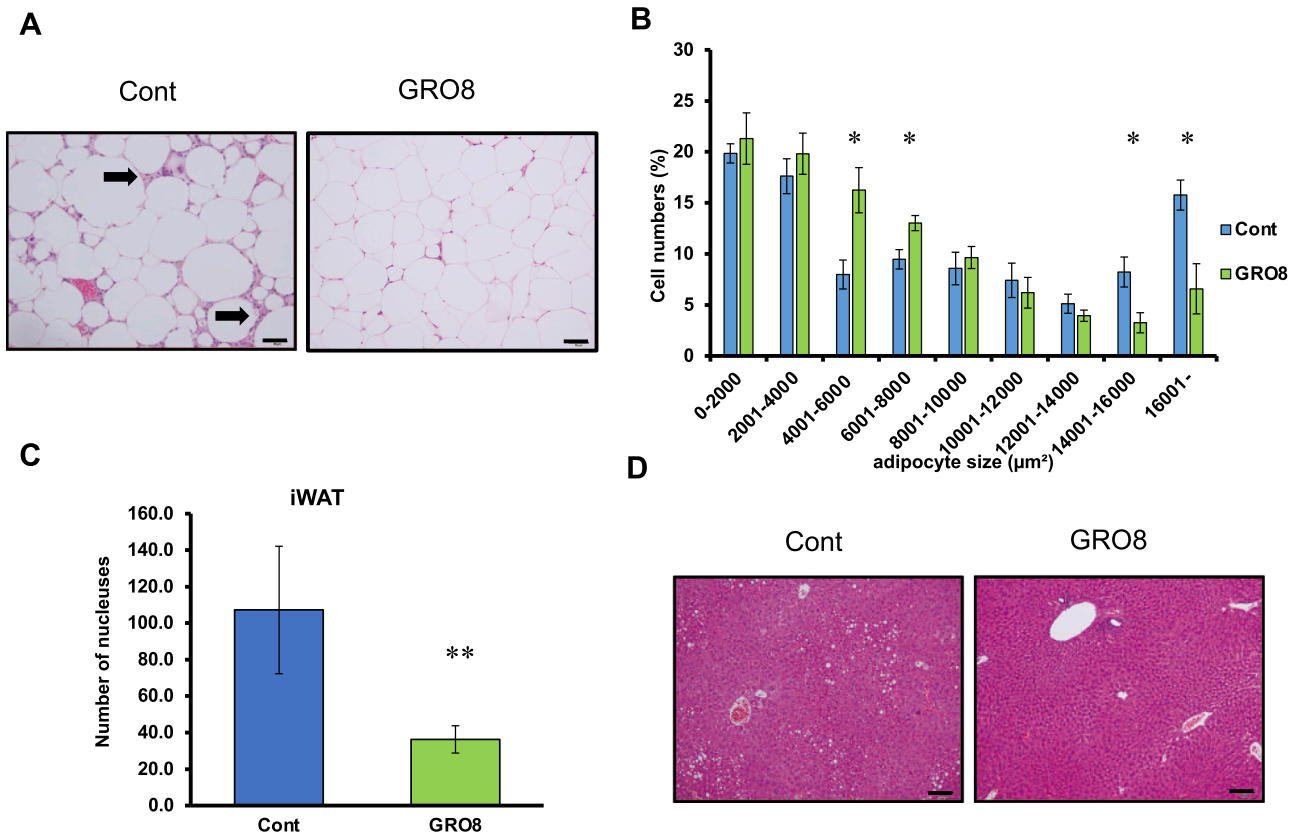

Fig. 4. GRO supplementation prevented hypertrophy of adipocytes in the iWAT of KK-A^y mice. (A) Images of iWAT stained with HE in 20-week-old KK-A^y mice. (B) Number of adipocytes in iWAT according to size. (C) Number of stromal vascular fraction cells in the iWAT of 20-week-old mice. (D) Images of the HE-stained liver of 20-week-old mice. Bar: 50 μm in (A) and (D); arrow: stromal vascular fraction including adipose macrophages in (A). Cont: control mice; GRO8: 0.8% GRO mice. The data were analyzed with one-way ANOVA followed by Tukey's test in (B) and Student's *t*-test in (C). *$p < 0.05$, **$p < 0.01$. Values are means $\pm$ SD (n = 5 per group, 5 fields per mouse were observed).
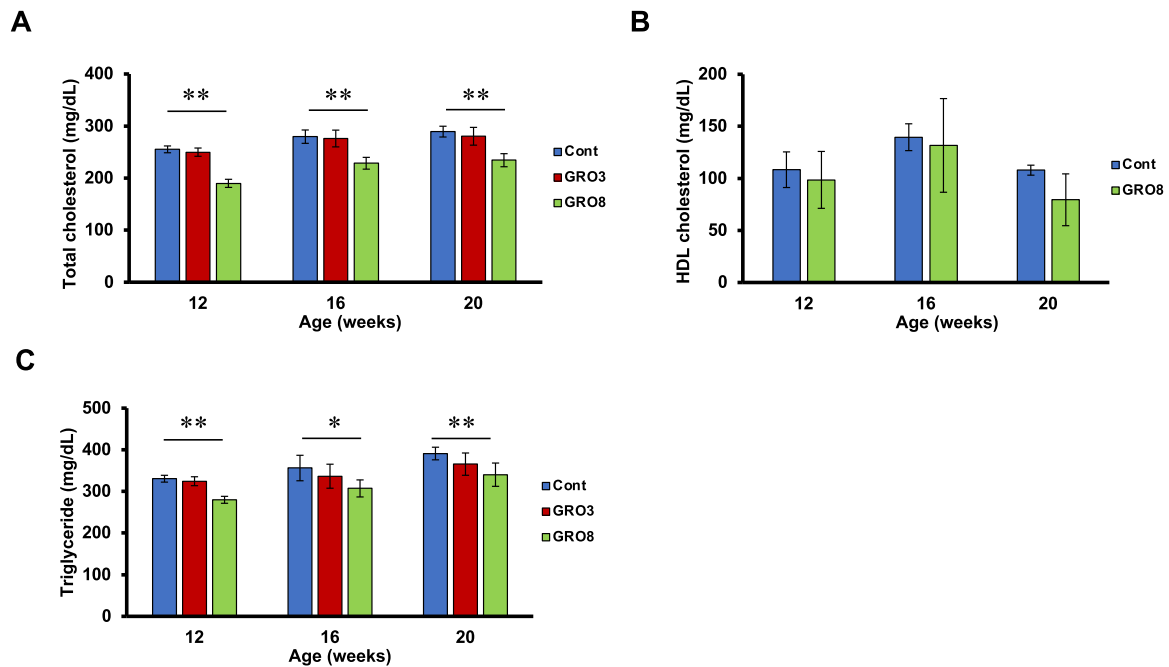
Fig. 5. GRO supplementation reduced the serum levels of total cholesterol and triglycerides in KK-A^y mice. Serum levels of (A) total cholesterol, (B) HDL, and (C) triglycerides. Cont: control mice; GRO3: 0.3% GRO mice; GRO8: 0.8% GRO mice. The data were analyzed with two-way ANOVA for independent variables, and subsequent one-way ANOVA followed by Tukey's test was performed for multiple comparisons. *$p < 0.05$, **$p < 0.01$. Values are means ± SD (n = 5).

verified the significant reduction in *Scd1* expression, to 20% of the Cont group level, in the 0.8% GRO group ($p < 0.001$) (Figs. 8A, and S1). In contrast, expression levels of *Fasn* and ChREBP/*Mlxipl* that are lipogenesis-related genes were not different between the two groups (Fig. S2). Next we evaluated the expression of genes that are related to *Scd1* and involved in lipid synthesis and fatty acid β-oxidation by qRT-PCR. The expression of cluster of differentiation 36 (*Cd36*), an integral membrane protein responsible for importing fatty acids into hepatocytes, was reduced by more than 50% in 0.8% GRO mice compared with Cont mice ($p < 0.001$). However, there was no difference in the expression of acetyl-CoA carboxylase-2 (*Acacb*/ACC-2), which catalyzes the intermediate rate-limiting step of fatty acid synthesis, between the 0.8% GRO and Cont groups. Enonyl-CoA hydratase and 3-hydroxyacyl CoA dehydrogenase (*Ehhadh*) a peroxisome enzyme involved in fatty acid β-oxidation, were ~ 50% lower in expression in 0.8% GRO compared with Cont mice ($p < 0.05$) (Fig. 8B). These changes in expression were not accompanied by changes in mitochondrial biogenesis mediators, including peroxisome proliferator-activated receptor gamma coactivator-α (PGC1α/*Ppargc1a*), -β (PGC1β/*Ppargc1b*), estrogen-related receptor α (*Erra*), and ATP synthase (*Atp5f1a*) as detected by RNA-seq (Supplemental Table 2) and qPCR (Fig. S3). Furthermore, we observed no significant difference in the expression of genes associated with fatty acid β oxidation, including very long chain acyl-CoA dehydrogenase (*Acadvl*), acyl-CoA oxidase 1 (*Acox1*), or medium chain acyl-CoA dehydrogenase (*Acadm*), which is involved in fatty acid oxidation.

As supplementation with 0.8% GRO improved glucose metabolism, the expression levels of genes regulating glucose metabolism were also evaluated by qRT-PCR. Among glycolysis-related genes, the expression of glucokinase (*Gck*), which phosphorylates glucose to form glucose-6-phosphate, was not different between 0.8% GRO and Cont mice; In contrast, that of pyruvate dehydrogenase kinase, isoenzyme 4 (*Pdk4*),

which regulates the pyruvate dehydrogenase (PDH) complex responsible for conversion of acetyl CoA from pyruvic acid, was reduced by more than 50% in 0.8% GRO mice compared with Cont mice ($p < 0.05$) (Fig. 8C). Among gluconeogenesis-related genes, the expression of phosphoenolpyruvate carboxykinase 1, cytosolic (*Pck1*), which converts oxaloacetate into phosphoenolpyruvate, was reduced by 0.8% GRO supplementation ($p = 0.05$), but the level of glucose-6-phosphatase, catalytic (*G6pc*), which synthesizes glucose from glucose 6-phosphate, was not changed (Fig. 8D).

The protein level of SCD1 in the liver was significantly reduced in 0.8% GRO mice compared with Cont mice, as determined by Western blot analysis (Fig. 9A). Although the mRNA level of PPARα was not affected, the protein level was significantly reduced by 0.8% GRO (Figs. 8A, and 9B). The ratio of phosphorylated AMPK to total AMPK was significantly higher in 0.8% GRO mice compared with Cont mice (Fig. 9C).

3.5. GRO supplementation changes a gene expression profile in the iWAT of KK-A^y mice

Since supplementation with 0.8% GRO reduced the iWAT weight, we compared the expression levels of genes regulating lipid and glucose metabolism in the iWAT between 0.8% GRO and Cont mice by qRT-PCR. Expression levels of *Scd1* and *Cd36*, which were decreased in the liver of 0.8% GRO mice, were not decreased in the iWAT (Fig. 10A). In contrast, the expression level of fatty acid synthase (FAS/*Fasn*) which catalyzes fatty acid synthesis, was decreased by ~ 50% in 0.8% GRO compared with Cont mice ($p < 0.05$) (Fig. 10A). The expression levels of glucose transporter 4 (*Glut4*), insulin receptor substrate 1 (*Irs1*), and carbohydrate-responsive element-binding protein (ChREBP/*Mlxipl*) were not different between the 0.8% GRO and Cont mice (Fig. 10B). Also, expression levels of glycolysis-related genes, *Gck* and *Pdk4* were
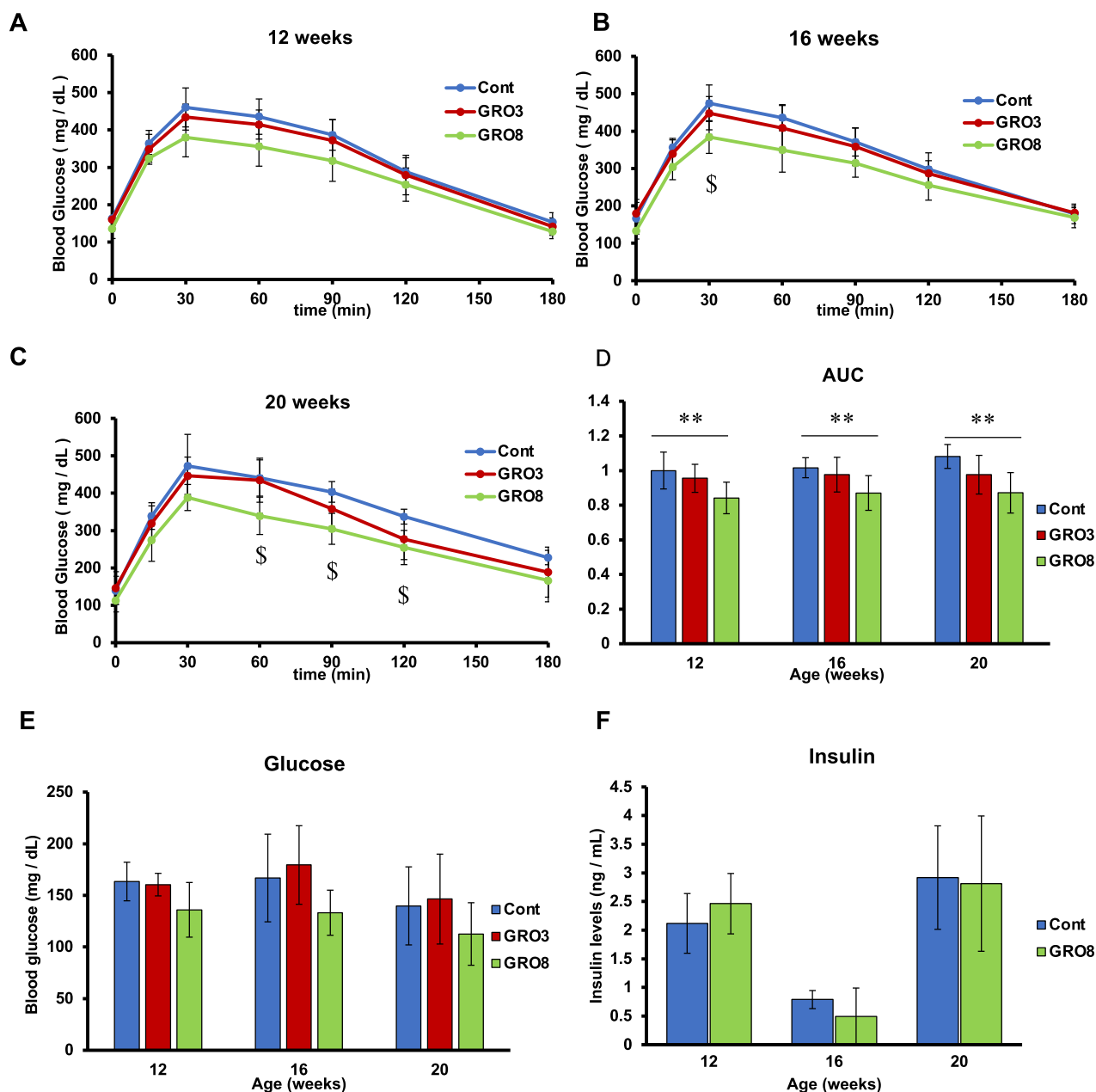
Fig. 6. GRO supplementation improved glucose metabolism. Changes in blood glucose levels after intraperitoneal injection of glucose (1 g/kg body weight) following 12 h of fasting in (A) 12-week-old mice, (B) 16-week-old mice, and (C) 20-week-old mice. (D) Area under the curve for the blood glucose level after intraperitoneal injection of glucose. (E) Serum glucose levels after 12 h of fasting. (F) Serum insulin levels after 12 h of fasting. Cont: control mice; GRO3: 0.3% GRO mice; GRO8: 0.8% GRO mice. The data were analyzed with two-way ANOVA for independent variables, and subsequent one-way ANOVA followed by Tukey's test was performed for multiple comparisons. $p < 0.05$ Cont vs. GRO8 in (B, C) and **$p < 0.01$ in (D). Graphs show the fold change in the area under the curve for 12-week-old mice relative to Cont mice. Values are means $\pm$ SD (n = 5).
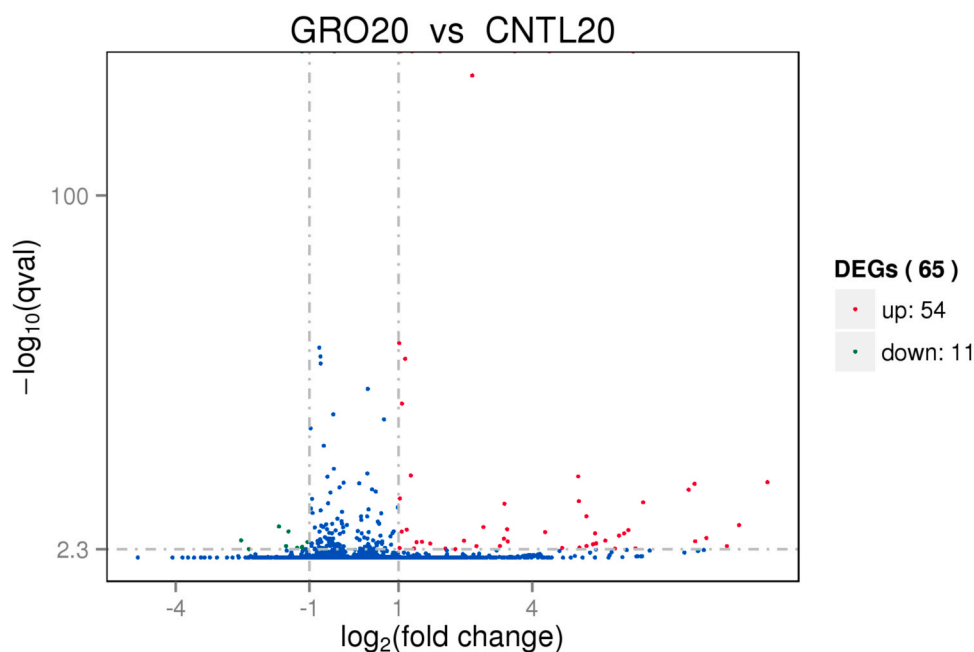
Fig. 7. GRO supplementation induced differential expression of genes in the liver, as determined by RNA-Seq analysis. A volcano plot is shown for the differentially expressed genes (DEGs) in the liver of 20-week-old 0.8% GRO mice (GRO20) versus Cont mice (CNTL20). The y-axis shows the mean log10 q-value, and the x-axis shows the mean log2 fold change. The blue dots indicate no statistically significant difference in expression ($q > 0.05$), whereas the red and green dots represent significantly upregulated and downregulated genes in GRO20 compared with CNTL20, respectively ($q < 0.05$); 54 genes were upregulated and 11 downregulated. (For interpretation of the references to color in this figure legend, the reader is referred to the web version of this article.)

Table 2

Gene ontology analysis of differentially expressed genes identified by RNA-Seq analysis.

GO_accession	Description	Term_type	Over_represented p-value	Corrected p-value	DEG item	DEG list
GO:0072359	Circulatory system development	biological_process	1.15E-05	0.003148	11	62
GO:0033993	Response to lipid	biological_process	0.000365	0.04558	9	62
GO:0006631	Fatty acid metabolic process	biological_process	0.000374	0.04633	6	62
GO:0010885	Regulation of cholesterol storage	biological_process	0.000393	0.047641	2	62

Table 3

Genes involved in lipid and glucose metabolism that were significantly ($p < 0.05$) differentially expressed between control and 0.8% GRO pooled liver samples, identified by RNA-Seq analysis.

| Gene_ID	Gene name	Gene description	Read counts Cont	GRO8	p-value
ENSMUSG00000042010	*Acacb*	acetyl-Coenzyme A carboxylase beta	52.74	30.04	0.02479
ENSMUSG00000062908	*Acadm*	acyl-Coenzyme A dehydrogenase, medium chain	819.08	632.20	0.00016
ENSMUSG00000018574	*Acadvl*	acyl-Coenzyme A dehydrogenase, very long chain	229.64	137.66	0.00002
ENSMUSG00000020777	*Acox1*	acyl-Coenzyme A oxidase 1, palmitoyl	3274.60	2531.47	0.00000
ENSMUSG00000002944	*Cd36*	CD36 antigen	322.57	223.66	0.00039
ENSMUSG00000022853	*Ehhadh*	enoyl-Coenzyme A, hydratase / 3-hydroxyacyl Coenzyme A dehydrogenase	589.76	438.68	0.00017
ENSMUSG00000022383	*Ppara*	peroxisome proliferator activated receptor alpha	83.32	34.36	0.00002
ENSMUSG00000037071	*Scd1*	stearoyl-Coenzyme A desaturase 1	9158.02	4088.25	0.00000
ENSMUSG00000025153	*Fasn*	fatty acid synthase	80.17	74.68	0.94594
ENSMUSG00000078650	*G6pc*	glucose-6-phosphatase, catalytic	514.20	481.63	0.93102
ENSMUSG00000041798	*Gck*	glucokinase	106.27	112.05	0.40423
ENSMUSG00000005373	*Mlxipl*	MLX interacting protein-like	130.01	136.51	0.37491
ENSMUSG00000027513	*Pck1*	phosphoenolpyruvate carboxykinase 1, cytosolic	4462.48	3269.65	0.00000
ENSMUSG00000019577	*Pdk4*	pyruvate dehydrogenase kinase, isoenzyme 4	20.39	38.95	0.00790
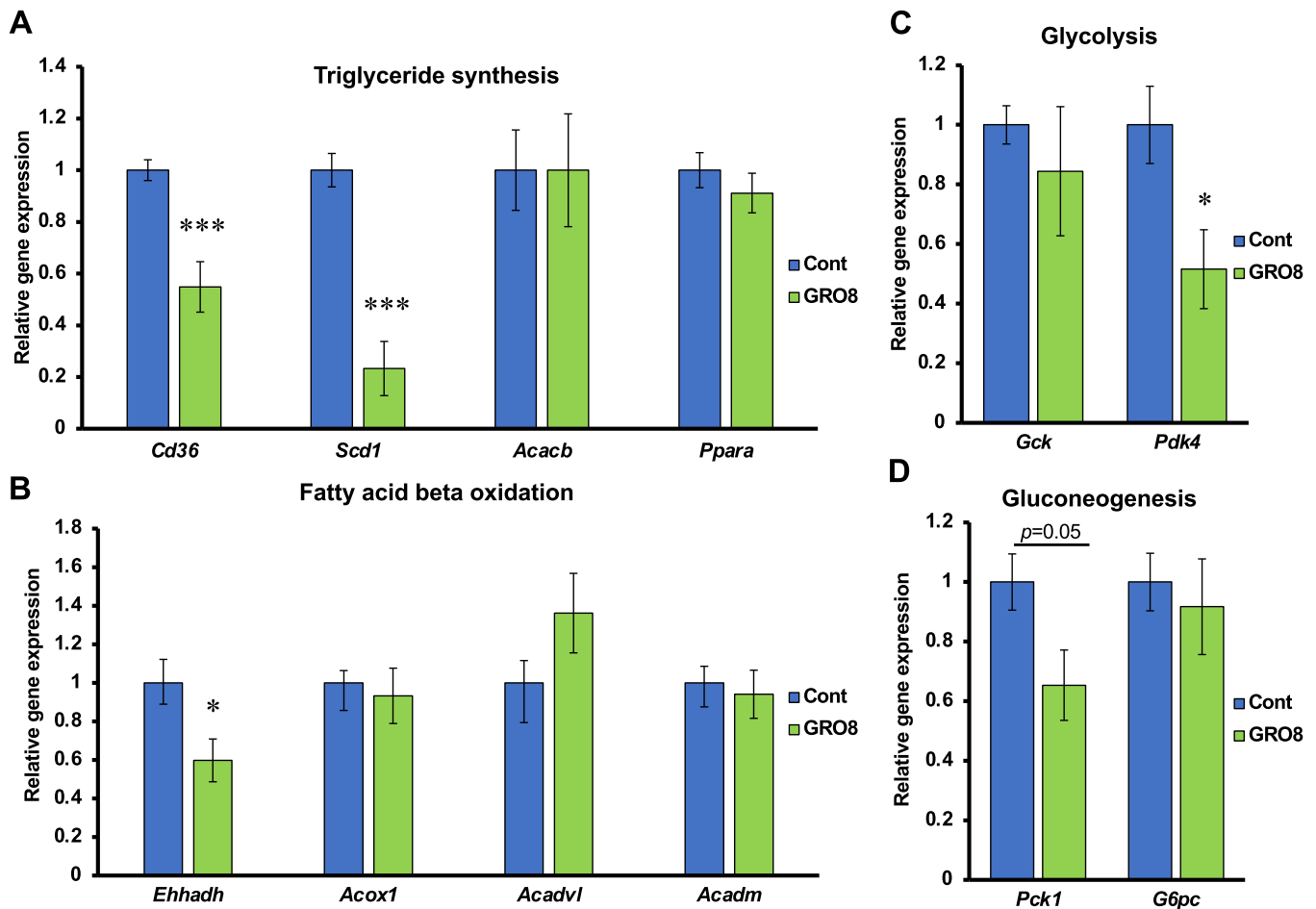
Fig. 8. GRO supplementation reduced the expression of enzymes related to triglyceride biosynthesis in the liver. Expression of genes involved in (A) triglyceride biosynthesis, (B) glycolysis, (C) ß-oxidation of fatty acids, and (D) gluconeogenesis in the liver of 20-week-old KK-A^y mice in the Cont and GRO8 groups, as determined by qRT-PCR. Graphs show the fold changes in mRNA levels normalized with respect to β-actin in the GRO8 mice relative to Cont mice. Cont: control mice; GRO8: 0.8% GRO mice. The data were analyzed with Student's t-test. $*p < 0.05$, $***p < 0.001$. Values are means $\pm$ SD (n = 5).

not different between the 0.8% GRO and Cont mice (Fig. S2). qRT-PCR analysis of inflammatory cytokines (adipokines) in iWAT revealed significantly reduced expression of interleukin 6 (*Il6*) in 0.8% GRO mice compared with Cont mice ($p < 0.05$) (Fig. 10C); however, expression of tumor necrosis factor α (*Tnf*) and the macrophage marker adhesion G protein-coupled receptor E1 (*Adgre1*) was unaffected by 0.8% GRO supplementation. Together, these results indicate that 0.8% GRO supplementation mitigated obesity partially by reducing lipogenesis and inflammation in the iWAT.

4. Discussion

In this study, we demonstrated the health-promoting effects of continuous and long-term supplementation of GRO using KK-A^y mice, a model of mild obesity and type 2 diabetes. Supplementation with 0.8% GRO mitigated increase in body weight and fat accumulation without affecting food intake. Furthermore, 0.8% GRO supplementation improved the blood lipid profile and glucose tolerance. More importantly, we gained insights into the molecular basis of the health-promoting effects of GRO. Thus, we revealed that the expression levels

of *Scd1*, and other genes associated with the lipid and glucose metabolism including *Cd36*, *Ehhadh*, *Pdk4*, and *Pck1* were significantly reduced in the liver of mice fed the 0.8% GRO diet for 12 weeks. In addition, we found that *Fasn* and *Il6* genes was downregulated in the iWAT of 0.8% GRO mice. Our results suggest that GRO supplementation improves lipid profiles by reducing de novo lipogenesis in the liver and white adipose tissue, in addition to improving glucose metabolism via increases in glycolysis in the liver (Fig. 11).

To elucidate the molecular pathway by which GRO mitigates obesity, we evaluated the effects of GRO on liver gene expression (Table 3) by RNA-Seq analysis followed by qRT-PCR. We found that the expression levels of *Cd36*, *Scd1*, *Ehhadh*, *Pdk4*, and *Pck1* were significantly reduced in the liver of mice fed the 0.8% GRO diet for 12 weeks. In particular, *Scd1* showed the greatest decrease in expression in the liver of 0.8% GRO mice (~ 20% of the Cont group level). We consider that the drastic reduction of the *Scd1* expression in the liver is one of the leys to the health-promoting effects of GRO. SCD1, the rate-limiting enzyme in MUFA and triglyceride syntheses in the liver, desaturates fatty acids into MUFAs such as oleate and palmitoleate. Thus, SCD1 is a central regulator of energy metabolism and of obesity and related metabolic diseases
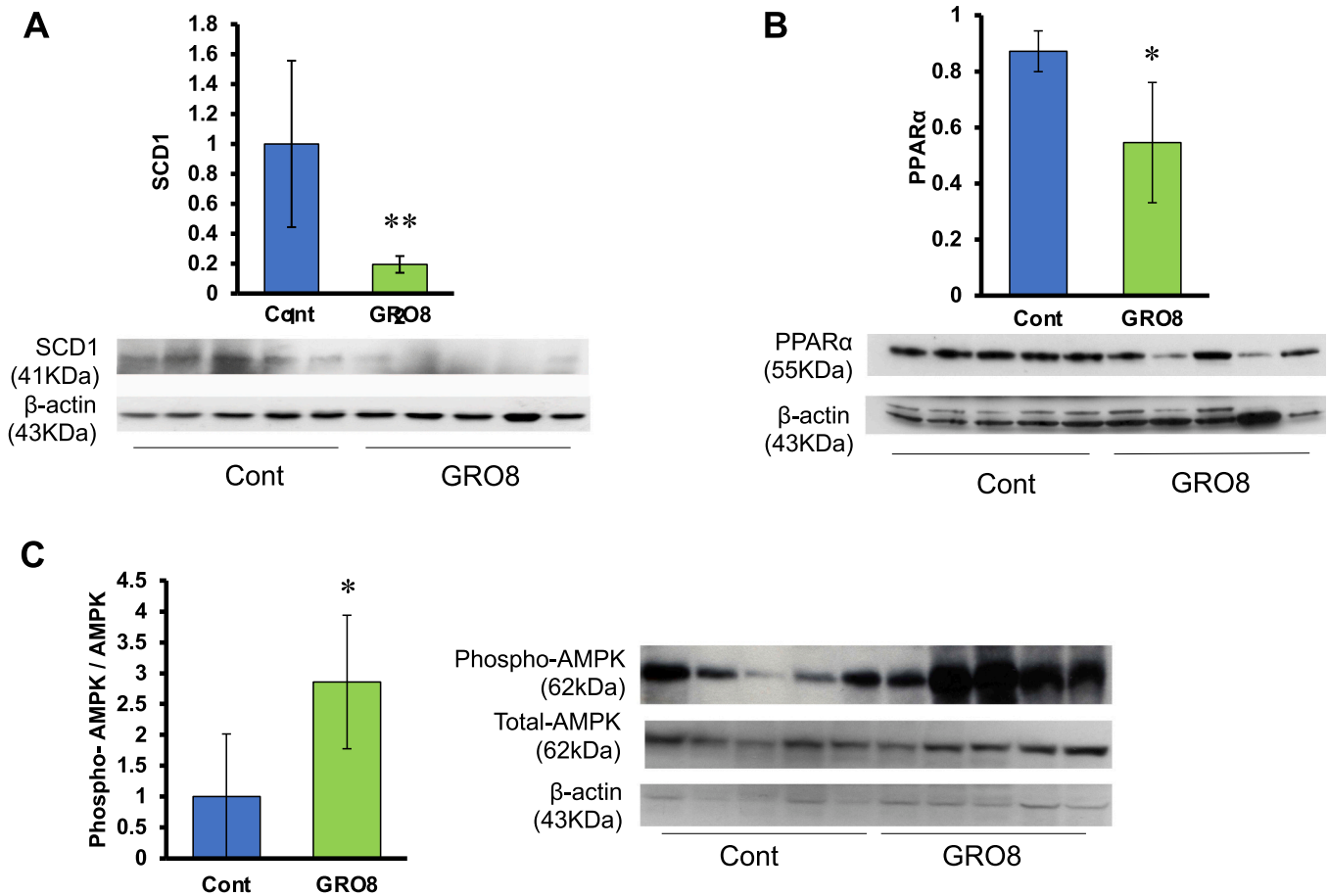
Fig. 9. GRO supplementation reduced the protein levels of SCD1 and PPARα and increased the level of phosphorylated AMPK in the liver. (A) Western blot analysis of SCD1 in the liver of 20-week-old mice. (B) Western blot analysis of PPARα in the liver of 20-week-old mice. (C) The ratio of phosphorylated AMPK to total AMPK levels in the liver of 20-week-old mice, as determined by Western blot analysis. Cont: control mice; GRO8: 0.8% GRO mice. The data were analyzed with Student's t-test. $*p < 0.05$, $*p < 0.01$. Values are means $\pm$ SD (n = 5).

including type 2 diabetes. Consistent with our results, prior studies demonstrated that systemic knockout or antisense oligonucleotide-mediated inhibition of *Scd1* prevented the increased body and white adipose tissue weights induced by a high-fat or high-carbohydrate diet in mice and rats [28–31], and in leptin-resistant/obese A^y/a mice [27]. *Scd1*-knockout or knockdown mice exhibited reduced hepatic expression of lipogenic genes including ACC2/*Acacb*, FAS/*Fasn*, sterol regulatory element binding transcription factor 1 (*Srebpf1*), and ELOVL family member 6, elongation of long chain fatty acids (*Elovl6*); however, the expression of these genes was not significantly reduced in GRO-treated mice, except for *Cd36*. In KK-A^y mice fed the GRO-supplemented diet, the expression of *Scd1* was reduced in the liver, but not iWAT. In mice with liver-specific knockout of *Scd1*, body and white adipose tissue weights, serum triglyceride levels, and lipogenic gene expression levels were reduced after feeding a high-carbohydrate/very-low-fat diet, but not a normal chow or high-fat diet [32].

GRO-treated mice exhibited lower body weight and decreased iWAT volume compared to animals fed the control diet, although food intake was not changed. In addition, gene expression levels of *Cd36*, a major player in lipid uptake, in iWAT were unchanged, suggesting that the lean phenotype might have resulted from alterations in basal thermogenesis, physical energy expenditure and/or energy absorption within the gastrointestinal tract rather than reduced fat storage in iWAT. Although we did not measure these variables in this study, *Scd1*-deficient mice exhibit upregulation in basal thermogenesis [33] and reduced hepatic de

novo lipogenesis that resulted in elevated levels of fatty acid oxidation mediated by the AMP-activated protein kinase (AMPK) pathway [34, 35].

The mechanism or pathway by which GRO reduces expression of SCD1 and related genes was not elucidated in this study. Many molecules including the liver X receptor (LXR), SREBP-1c/SREBPF1, ChREBP/MLXIPL, PPARα, and PPARγ regulate the expression of SCD1 [36]. However, we did not observe significant differences in the expression levels of these genes between the 0.8% GRO and Cont mice (data not shown). Regardless, RNA-Seq and gene ontology analyses of the differentially expressed genes after GRO supplementation suggested a role of PPARα pathways. In addition, Western blot revealed a lower protein level in 0.8% GRO compared with Cont mice. Previous work using primary rat hepatocyte has shown that the expression of hepatic *Scd1* and *Fasn* are directly regulated by PPARα during re-feeding state [37]. Thus, although it is still lack of restoration experiments with PPARα expression, we suggest that GRO mediates hepatic lipid metabolisms in a PPARα-dependent manner.

We observed a significant improvement in glucose tolerance or the levels of fasting blood glucose in GRO-supplemented mice. *Scd1*-knockout mice fed a high-fat diet and hepatocyte-specific *Scd1*-knockout mice fed a high-carbohydrate diet showed improved glucose tolerance and reduced gluconeogenesis and glycolysis; in addition, the expression of *Pck1* was reduced in the liver of the *Scd1*-knockout mice [31]. In this study, supplementation of 0.8% GRO significantly reduced the expression of *Pck1* and glycolysis-related *Pdk4*. In liver-specific *Scd1*-knockout
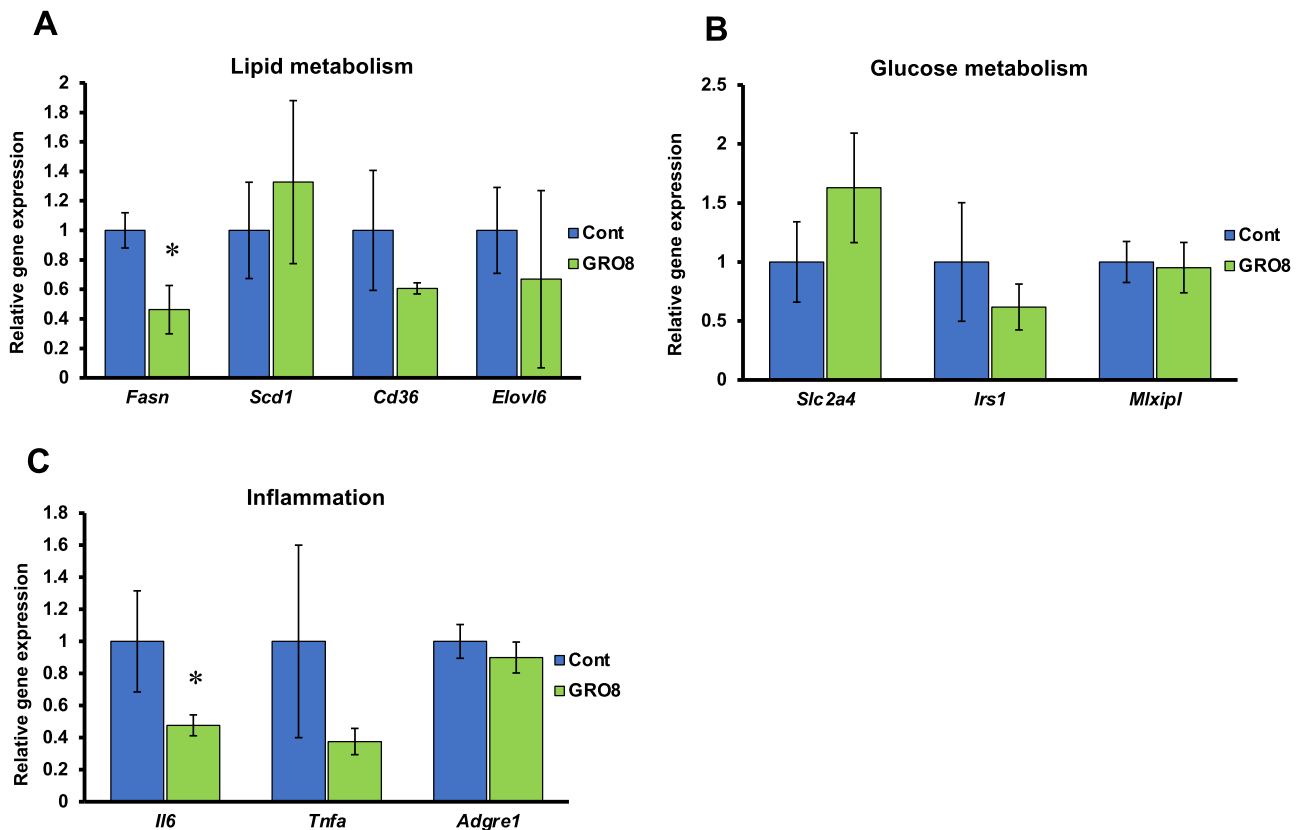
Fig. 10. GRO supplementation reduced the expression of genes related to lipid metabolism and inflammation in iWAT. (A) Expression of genes related to lipid metabolism in the iWAT of 20-week-old KK-A^y mice in the Cont and 0.8% GRO groups were compared by qRT-PCR. Genes related to (B) glucose metabolism and (C) inflammation. Graphs show the fold changes in normalized mRNA levels relative to those of 20-week-old mice in the Cont group. Cont: control mice; GRO8: 0.8% GRO mice. The data were analyzed with Student's t-test. $*p < 0.05$. Values are means $\pm$ SD (n = 5).

mice fed a high-carbohydrate diet, mitochondrial gene expression and ATP consumption were induced and led to reductions in gluconeogenesis and glycolysis [32]. RNA-seq and qRT-PCR assays indicated that expression of PGC-1α/Ppargc1a, a regulator of mitochondrial biogenesis, was not affected (Fig. S3), whereas that of Ehhadh, related to fatty acid ß-oxidation, was reduced in 0.8% GRO compared with Cont mice. Although our data examined gene expression only at a transcriptional level, this might suggest decreased ß-oxidation of fatty acids in 0.8% GRO mice. In addition, the expression of Pdk4 was significantly lower in 0.8% GRO compared with Cont mice. PDK4 is a negative regulator of PDH [38], which catalyzes the conversion of pyruvate to acetyl CoA. Reduced expression or inactivation of PDH accelerated gluconeogenesis, impaired glucose metabolism and aggravated type 2 diabetes [39,40], whereas Pdk4 knockout improved glucose tolerance in a diabetic model mouse [41,42]. In addition, increased ß-oxidation of fatty acids was reported to decrease PDH activity [40]. Thus, the reduced expression of Pdk4 and ß-oxidation of fatty acids observed in 0.8% GRO mice may amplify PDH activity and decrease gluconeogenesis (Fig. 8).

In iWAT, we observed reduced expression of lipogenic FAS/Fasn, but no significant change in the mRNA expression of Scd1 or glucose metabolism-related genes. Interestingly, the expression of a major adipokine, Il6, was repressed in the iWAT of the 0.8% GRO mice. Although we could not detect reduced expression of the macrophage marker F4/80 /Adgre1 by qRT-PCR, we observed fewer stromal vascular fraction cells, including adipose tissue macrophages, in the iWAT of the 0.8% GRO (Fig. 4A, C). The reduction of these ell population might be responsible for the reduction in the Il expression level. The suppression of proinflammatory adipokine expression enhances insulin sensitivity and the metabolic abnormalities associated with obesity and diabetes [43,44].

Several molecular mechanisms of the beneficial health effects of products containing glabridin, a major constituent of GRO, have been postulated. Among them, activation of the AMPK pathway is the most widely recognized, especially in muscle [20,21]. Glabridin treatment (150 mg/kg/day) for 4 weeks in C57Bl/6J mice fed a high-fat diet decreased body weight, and fat accumulation and improved glucose metabolism. In the mice, glabridin treatment increased the ratio of phosphorylated AMPK/total AMPK in the liver, iWAT, and muscles and suppressed the expression of Srebpf1, Fasn, Acacb, Scd1, and Pck1 in the liver and Srebpf1, Fasn, Acacb, and Scd1 in iWAT [45]. However, 0.8% GRO treatment did not suppress expression of Fasn or Acacb in the liver or expression of Scd1 in the iWAT. We also observed an increased phosphorylated AMPK/total AMPK ratio in the liver of the 0.8% GRO mice. Although glabridin treatment has been reported to improve glucose metabolism and enhance muscle mass in KK-A^y mice [20,46], we observed a significant increase in the quadriceps weight relative to body weight only and could not confirm an increase in muscle mass induced by GRO supplementation.

A recent preliminary report involving small numbers of healthy individuals and patients with type 2 diabetes reported health-promoting effects of glabridin treatment in the healthy individuals but very subtle effects in the patients and suggested the value of glabridin as a preventive supplement for healthy individuals [47]. The underlying molecular mechanisms by which GRO supplementation mitigates obesity and insulin resistance are complex and were not completely elucidated here. However, future systemic investigations focusing on the crosstalk among the liver, adipose tissue, and muscle [46,48,49] may provide useful information for using GRO to prevent and treat metabolic syndromes and diabetes.
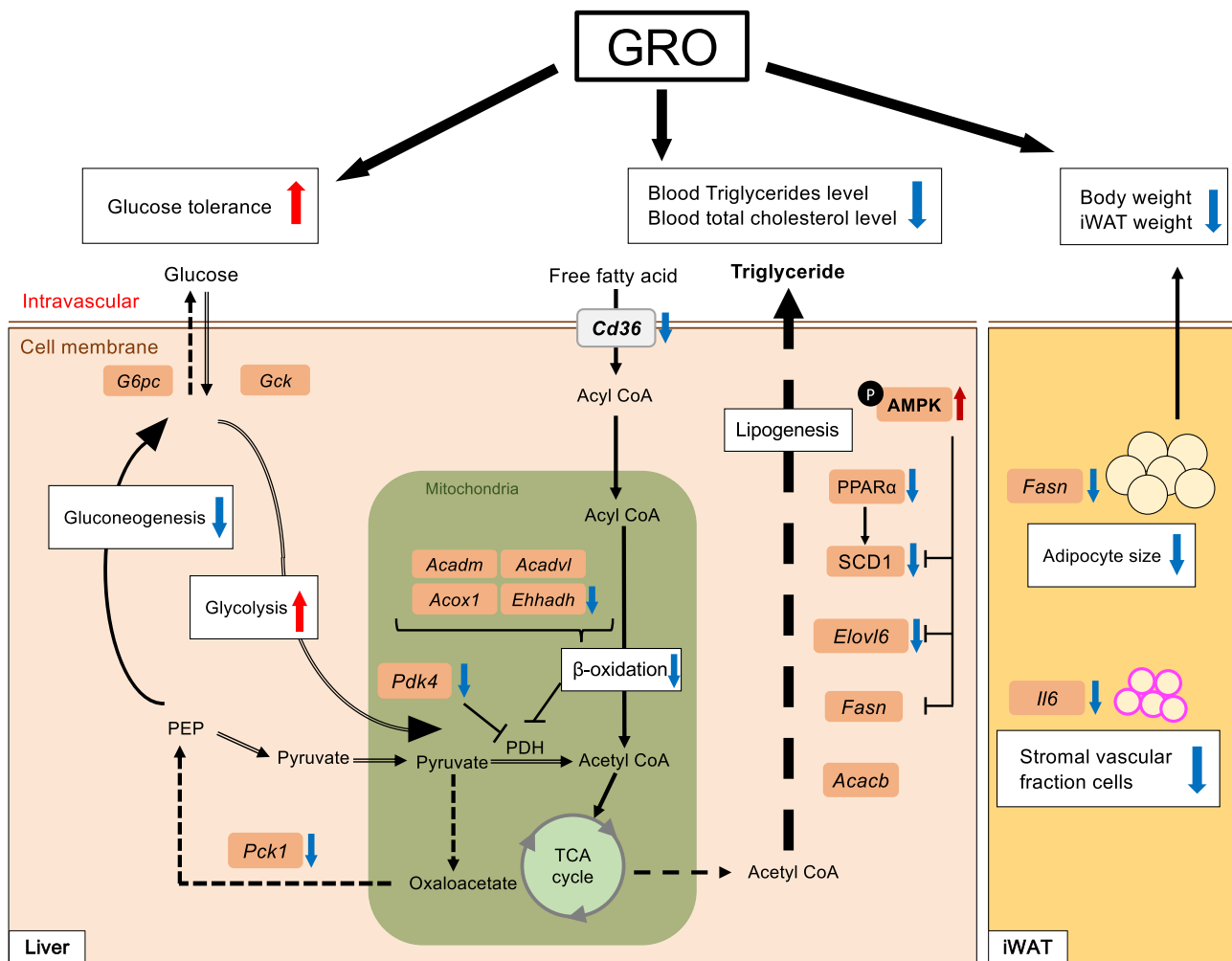
Fig. 11. Proposed mechanism by which GRO improves glucose metabolism and blood lipid profiles while decreasing obesity in KK-A^y mice. In the liver, GRO reduced gluconeogenesis thorough reduction of *Pck1* gene expression and increased glycolysis through downregulation of *Pdk4* gene expression. Decreased glucose blood secretion and activation of the glycolysis pathway could lead to improved glucose tolerance. GRO supplementation reduced *Pdk4* expression that in turn down-regulates PDH, an enzyme that mediates glycolytic pathways in mitochondria. Moreover, expression levels of *Ehhadh*, an enzyme in the fatty acid β-oxidation pathway, were reduced. Protein expression levels of the lipogenesis-mediated enzyme SCD1, which is regulated at a transcriptional level by PPARα, were significantly decreased. Phosphorylation of AMPK was activated and in turn expression of its target *Elovl6* was decreased. The weight of iWAT and adipocyte size were significantly decreased and levels of the lipogenic enzyme *Fasn* were also decreased. As the area of the cells in the stromal vascular fraction decreased, expression levels of IL-6, an inflammation marker, decreased.

Conflict of interest statement

The authors declare that there are no conflicts of interest.

Appendix A. Supplementary material

Supplementary data associated with this article can be found in the online version at doi:10.1016/j.biopha.2021.111714.

References

[1] P.G. Kopelman, Obesity as a medical problem, Nature 404 (2000) 635–643.
[2] P. Zimmet, Globalization, coca-colonization and the chronic disease epidemic: can the Doomsday scenario be averted? J. Intern. Med. 247 (2000) 301–310.
[3] P. Zimmet, K.G. Alberti, J. Shaw, Global and societal implications of the diabetes epidemic, Nature 414 (2001) 782–787.
[4] B.B. Lowell, G.I. Shulman, Mitochondrial dysfunction and type 2 diabetes, Science 307 (2005) 384–387.
[5] P. Dandona, A. Aljada, A. Bandyopadhyay, Inflammation: the link between insulin resistance, obesity and diabetes, Trends Immunol. 25 (2004) 4–7.
[6] Y. Yagishita, A. Uruno, T. Fukutomi, R. Saito, D. Saigusa, J. Pi, A. Fukamizu, F. Sugiyama, S. Takahashi, M. Yamamoto, Nrf2 improves leptin and insulin resistance provoked by hypothalamic oxidative stress, Cell Rep. 18 (2017) 2030–2044.
[7] J. Ye, Mechanisms of insulin resistance in obesity, Front. Med. 7 (2013) 14–24.
[8] A.J. Cruz-Jentoft, A.A. Sayer, Sarcopenia, Lancet 393 (2019) 2636–2646.
[9] S. Shibata, A drug over the millennia: pharmacognosy, chemistry, and pharmacology of licorice, Yakugaku Zasshi 120 (2000) 849–862.
[10] M. Kuroda, Y. Mimaki, Y. Sashida, T. Mae, H. Kishida, T. Nishiyama, M. Tsukagawa, E. Konishi, K. Takahashi, T. Kawada, K. Nakagawa, M. Kitahara, Phenolics with PPAR-gamma ligand-binding activity obtained from licorice (Glycyrrhiza uralensis roots) and ameliorative effects of glycyrin on genetically diabetic KK-A(y) mice, Bioorg. Med. Chem. Lett. 13 (2003) 4267–4272.
[11] T.Y. Wu, T.O. Khor, C.L. Saw, S.C. Loh, A.I. Chen, S.S. Lim, J.H. Park, L. Cai, A. N. Kong, Anti-inflammatory/anti-oxidative stress activities and differential

regulation of Nrf2-mediated genes by non-polar fractions of tea Chrysanthemum zawadskii and licorice Glycyrrhiza uralensis, AAPS J. 13 (2011) 1–13.

[12] H. Haraguchi, N. Yoshida, H. Ishikawa, Y. Tamura, K. Mizutani, T. Kinoshita, Protection of mitochondrial functions against oxidative stresses by isoflavans from Glycyrrhiza glabra, J. Pharm. Pharmacol. 52 (2000) 219–223.

[13] T. Fukai, A. Marumo, K. Kaitou, T. Kanda, S. Terada, T. Nomura, Anti-Helicobacter pylori flavonoids from licorice extract, Life Sci. 71 (2002) 1449–1463.

[14] C.K. Lee, K.K. Park, S.S. Lim, J.H. Park, W.Y. Chung, Effects of the licorice extract against tumor growth and cisplatin-induced toxicity in a mouse xenograft model of colon cancer, Biol. Pharm. Bull. 30 (2007) 2191–2195.

[15] K. Nakagawa, M. Kitano, H. Kishida, T. Hidaka, K. Nabae, M. Kawabe, K. Hosoe, 90-Day repeated-dose toxicity study of licorice flavonoid oil (LFO) in rats, Food Chem. Toxicol. 46 (2008) 2349–2357.

[16] K. Nakagawa, H. Kishida, N. Arai, T. Nishiyama, T. Mae, Licorice flavonoids suppress abdominal fat accumulation and increase in blood glucose level in obese diabetic KK-A(y) mice, Biol. Pharm. Bull. 27 (2004) 1775–1778.

[17] F. Aoki, S. Honda, H. Kishida, M. Kitano, N. Arai, H. Tanaka, S. Yokota, K. Nakagawa, T. Asakura, Y. Nakai, T. Mae, Suppression by licorice flavonoids of abdominal fat accumulation and body weight gain in high-fat diet-induced obese C57BL/6J mice, Biosci. Biotechnol. Biochem. 71 (2007) 206–214.

[18] Y. Tominaga, K. Nakagawa, T. Mae, M. Kitano, S. Yokota, T. Arai, H. Ikematsu, S. Inoue, Licorice flavonoid oil reduces total body fat and visceral fat in overweight subjects: a randomized, double-blind, placebo-controlled study, Obes. Res. Clin. Pract. 3 (2009) I–IV.

[19] M. Kuroda, Y. Mimaki, S. Honda, H. Tanaka, S. Yokota, T. Mae, Phenolics from Glycyrrhiza glabra roots and their PPAR-gamma ligand-binding activity, Bioorg. Med. Chem. 18 (2010) 962–970.

[20] Y. Yoshioka, Y. Yamashita, H. Kishida, K. Nakagawa, H. Ashida, Licorice flavonoid oil enhances muscle mass in KK-A(y) mice, Life Sci. 205 (2018) 91–96.

[21] K. Sawada, Y. Yamashita, T. Zhang, K. Nakagawa, H. Ashida, Glabridin induces glucose uptake via the AMP-activated protein kinase pathway in muscle cells, Mol. Cell. Endocrinol. 393 (2014) 99–108.

[22] M. Nishimura, Breeding of mice strains for diabetes mellitus, Exp. Anim. 18 (1969) 147–157.

[23] A.J. King, The use of animal models in diabetes research, Br. J. Pharmacol. 166 (2012) 877–894.

[24] Z. Xu, J. Huo, X. Ding, M. Yang, L. Li, J. Dai, K. Hosoe, H. Kubo, H. Mori, K. Higuchi, J. Sawashita, Coenzyme Q10 improves lipid metabolism and ameliorates obesity by regulating CaMKII-mediated PDE4 inhibition, Sci. Rep. 7 (2017) 8253.

[25] M. Kitada, Y. Ogura, D. Koya, Rodent models of diabetic nephropathy: their utility and limitations, Int. J. Nephrol. Renov. Dis. 9 (2016) 279–290.

[26] S.A. Bustin, V. Benes, J. Garson, J. Hellemans, J. Huggett, M. Kubista, R. Mueller, T. Nolan, M.W. Pfaffl, G. Shipley, C.T. Wittwer, P. Schjerling, P.J. Day, M. Abreu, B. Aguado, J.F. Beaulieu, A. Beckers, S. Bogaert, J.A. Browne, F. Carrasco-Ramiro, L. Ceelen, K. Ciborowski, P. Cornillie, S. Coulon, A. Cuypers, S. De Brouwer, L. De Ceuninck, J. De Craene, H. De Naeyer, W. De Spiegelaere, K. Deckers, A. Dheedene, K. Durinck, M. Ferreira-Teixeira, A. Fieuw, J.M. Gallup, S. Gonzalo-Flores, K. Goossens, E. Heindryckx, E. Herring, H. Hoenicka, L. Icardi, R. Jaggi, F. Javad, M. Karampelias, F. Kibenge, M. Kibenge, C. Kumps, I. Lambertz, T. Lammens, A. Markey, P. Messiaen, E. Mets, S. Morais, A. Mudarra-Rubio, J. Nakiwala, H. Nelis, P.A. Olsvik, C. Pérez-Novo, M. Plusquin, T. Remans, A. Rihani, P. Rodrigues-Santos, P. Rondou, R. Sanders, K. Schmidt-Bleek, K. Skovgaard, K. Smeets, L. Tabera, S. Toegel, T. Van Acker, W. Van den Broeck, J. Van der Meulen, M. Van Gele, G. Van Peer, M. Van Poucke, N. Van Roy, S. Vergult, J. Wauman, M. Tshuikina-Wiklander, E. Willems, S. Zaccara, F. Zeka, J. Vandesompele, The need for transparency and good practices in the qPCR literature, Nat. Methods 10 (2013) 1063–1067.

[27] M. Miyazaki, H. Sampath, X. Liu, M.T. Flowers, K. Chu, A. Dobrzyn, J.M. Ntambi, Stearoyl-CoA desaturase-1 deficiency attenuates obesity and insulin resistance in leptin-resistant obese mice, Biochem. Biophys. Res. Commun. 380 (2009) 818–822.

[28] J.M. Ntambi, M. Miyazaki, J.P. Stoehr, H. Lan, C.M. Kendziorski, B.S. Yandell, Y. Song, P. Cohen, J.M. Friedman, A.D. Attie, Loss of stearoyl-CoA desaturase-1

[29] function protects mice against adiposity, Proc. Natl. Acad. Sci. USA 99 (2002) 11482–11486.

[29] J.M. Ntambi, M. Miyazaki, Regulation of stearoyl-CoA desaturases and role in metabolism, Prog. Lipid Res. 43 (2004) 91–104.

[30] G. Jiang, Z. Li, F. Liu, K. Ellsworth, Q. Dallas-Yang, M. Wu, J. Ronan, C. Esau, C. Murphy, D. Szalkowski, R. Bergeron, T. Doebber, B.B. Zhang, Prevention of obesity in mice by antisense oligonucleotide inhibitors of stearoyl-CoA desaturase-1, J. Clin. Investig. 115 (2005) 1030–1038.

[31] R. Gutiérrez-Juárez, A. Pocai, C. Mulas, H. Ono, S. Bhanot, B.P. Monia, L. Rossetti, Critical role of stearoyl-CoA desaturase-1 (SCD1) in the onset of diet-induced hepatic insulin resistance, J. Clin. Investig. 116 (2006) 1686–1695.

[32] M. Miyazaki, M.T. Flowers, H. Sampath, K. Chu, C. Otzelberger, X. Liu, J. M. Ntambi, Hepatic stearoyl-CoA desaturase-1 deficiency protects mice from carbohydrate-induced adiposity and hepatic steatosis, Cell Metab. 6 (2007) 484–496.

[33] S.H. Lee, A. Dobrzyn, P. Dobrzyn, S.M. Rahman, M. Miyazaki, J.M. Ntambi, Lack of stearoyl-CoA desaturase 1 upregulates basal thermogenesis but causes hypothermia in a cold environment, J. Lipid Res. 45 (2004) 1674–1682.

[34] M.T. Flowers, J.M. Ntambi, Role of stearoyl-coenzyme A desaturase in regulating lipid metabolism, Curr. Opin. Lipidol. 19 (2014) 248–256.

[35] P. Dobrzyn, A. Dobrzyn, M. Miyazaki, P. Cohen, E. Asilmaz, D.G. Hardie, J. M. Friedman, J.M. Ntambi, Stearoyl-CoA desaturase 1 deficiency increases fatty acid oxidation by activating AMP-activated protein kinase in liver, Proc. Natl. Acad. Sci. USA 101 (2004) 6409–6414.

[36] A.L. AM, D.N. Syed, J.M. Ntambi, Insights into stearoyl-CoA desaturase-1 regulation of systemic metabolism, Trends Endocrinol. Metab. 28 (2017) 831–842.

[37] A.M. Hebbachi, B.L. Knight, D. Wiggins, D.D. Patel, G.F. Gibbons, Peroxisome proliferator-activated receptor α deficiency abolishes the response of lipogenic gene expression to re-feeding, Biol. Chem. 283 (2008) 4866–4876.

[38] S. Zhang, M.W. Hulver, R.P. McMillan, M.A. Cline, E.R. Gilbert, The pivotal role of pyruvate dehydrogenase kinases in metabolic flexibility, Nutr. Metab. 11 (2014) 10 (Lond.).

[39] J.E. Foley, Rationale and application of fatty acid oxidation inhibitors in treatment of diabetes mellitus, Diabetes Care 15 (1992) 773–784.

[40] L. Hue, H. Taegtmeyer, The Randle cycle revisited: a new head for an old hat, Am. J. Physiol. Endocrinol. Metab. 297 (2009) E578–E591.

[41] B. Hwang, N.H. Jeoung, R.A. Harris, Pyruvate dehydrogenase kinase isoenzyme 4 (PDHK4) deficiency attenuates the long-term negative effects of a high-saturated fat diet, Biochem. J. 423 (2009) 243–252.

[42] R. Tao, X. Xiong, R.A. Harris, M.F. White, X.C. Dong, Genetic inactivation of pyruvate dehydrogenase kinases improves hepatic insulin resistance induced diabetes, PLoS One 8 (2013) 71997.

[43] S. Nishimura, I. Manabe, M. Nagasaki, K. Eto, H. Yamashita, M. Ohsugi, M. Otsu, K. Hara, K. Ueki, S. Sugiura, K. Yoshimura, T. Kadowaki, R. Nagai, CD8+ effector T cells contribute to macrophage recruitment and adipose tissue inflammation in obesity, Nat. Med. 15 (2009) 914–920.

[44] H. Kwon, J.E. Pessin, Adipokines mediate inflammation and insulin resistance, Front. Endocrinol. 4 (2013) 71 (Lausanne).

[45] J.W. Lee, S.S. Choe, H. Jang, J. Kim, H.W. Jeong, H. Jo, K.H. Jeong, S. Tadi, M. G. Park, T.H. Kwak, J. Man Kim, D.H. Hyun, J.B. Kim, AMPK activation with glabridin ameliorates adiposity and lipid dysregulation in obesity, J. Lipid Res. 53 (2012) 1277–1286.

[46] Y. Yamashita, H. Kishida, K. Nakagawa, Y. Yoshioka, H. Ashida, Liquorice flavonoid oil suppresses hyperglycaemia accompanied by skeletal muscle myocellular GLUT4 recruitment to the plasma membrane in KK-A(y) mice, Int. J. Food Sci. Nutr. 70 (2019) 294–302.

[47] A. Hattori, M. Takemoto, T. Ishikawa, Y. Maezawa, M. Koshizaka, H. Tokuyama, P. He, H. Kawamura, K. Kobayashi, K. Yokote, Metabolic effects of glabridin in healthy volunteers and patients with type 2 diabetes: a pilot study, Cogent Food Agric. 5 (2019), 1665943.

[48] S.J. Wakil, L.A. Abu-Elheiga, Fatty acid metabolism: target for metabolic syndrome, J. Lipid Res. Suppl. 50 (2009) S138–S143.

[49] M. Roden, G.I. Shulman, The integrative biology of type 2 diabetes, Nature 576 (2019) 51–60.